Reservoir Studies and Structural Interpretation of 3-D Seismic Data over X-Field, Niger Delta

[1]Adeoye, T. O., [2]Sunmonu, L. A., [3]Adabanija, M. A., [4]Bayowa, O. G. and [5]Suleman, K.O.

[1]Geophysics Department, University of Ilorin, Nigeria.
[2]Department of Pure and Applied Physics, Ladoke Akintola University of Technology, Nigeria.
[3,4]Department of Earth Sciences, Ladoke Akintola University of Technology, Nigeria.
[5] Department of Physics, Nigeria Maritime University, Okerenkoko, Warri, Nigeria.

Corresponding Author: toadeoye@gmail.com

Abstract

Petrophysical analysis and structural interpretation are the essential starting methods for mapping the reservoir distribution. Structural models are developed in this study using 3-D seismic data and analysis of covariance attributes. Well logs and 3-D seismic data were analyzed to identify prolific hydrocarbon intervals. Fault interpretation was enhanced by interpreting vertical sections of covariance attribute. Two horizons, picked at the reservoir level were used for structural modelling. Reserves estimation was obtained at probabilistic levels. Results show that three hydrocarbon bearing reservoirs are present in the field. The prospects consist of vertically stacked oil-saturated sands having an average net thickness of 143 ft. At least two of the oil sands spread from well 3 in the south to other distant wells. In addition, covariance attributes increased the fault population as faults are not very prominent on the seismic data. The structural maps reveal that the area contains normal listric faults that are not extensive in the vertical and lateral direction and are mostly unconnected to one other. The anticlinal structures that can trap hydrocarbon fluids are located in the North. Even though, wells in the southern part of the area have penetrated oil sands, migration is towards the anticlinal structures observed in northern part of the area as there are no sufficient structures in the south. The study concludes that oil sands exist in the region, and they are located within good traps. The limited lateral extent of the first reservoir constrained its recoverable oil amount, estimated at an average value of 394,192 barrels. Nevertheless, the second reservoir is of a high volume, measured at an average estimate of 1,120,779 barrels. The third reservoir has low hydrocarbon saturation. Despite the fragmented fault networks, the substantial presence of valuable oil sands and promising trapping structures in the northern region emphasizes the considerable potential for an expanded exploration and development program within the field.

Keywords: Structural Interpretation, Petrophysical Analysis, Hydrocarbon Exploration, Reservoir, Niger Delta.

1. INTRODUCTION

Hydrocarbon exploration is a costly venture and making the wrong developmental decisions can hurt the expedition's chances of success. Both structural styles and fault patterns are major

factors that control the reservoir location, size, and quality (Adeoye *et al.*, 2022). Therefore, detail structural interpretation can be used to locate the hydrocarbon bearing reservoir, as well as determine its size. Essentially, this involves mapping geometric arrangement of rock that allows significant oil and gas volumes to accumulate in them. In essence, structural interpretation and well log analysis are frontrunner tools that can be employed as they help to probe the depth and spatial location of the reservoir when they are integrated (Coffen, 1984). Depending on the knowledge of the local geology, several approaches to locating the hydrocarbon medium may be employed. However, if exploration wells are drilled, a typical well-defined hydrocarbon search usually begins with petrophysical analysis of the well log data (Adeoye *et al*, 2017). Different geophysical well log signatures are connected to the search for oil and gas, for example, the gamma ray, resistivity, and porosity logs are usually the best to be carefully analyzed, in order to quickly identify the hydrocarbon intervals in the subsurface (Adeoye *et al*, 2018). To obtain the understanding of the spatial location of the hydrocarbon system, contour maps are commonly generated to locate the trapping mechanism and aerial extent of the reservoir (Ashcroft, 2011). In order to generate this type of diagram, it is important to effectively pick key horizons on a good number of the seismic lines within the survey. This is usually combined with fault interpretation if there are faults in the field of study. Learning how to select important horizons, contour the data, and visualize them in three dimensions, effectively are critical skills for mapping the subsurface. This is particularly essential due to the complexities posed by stratigraphic changes, such as facies shifts, or vertical and lateral discontinuities like unconformities. These variations can make the mapping of relevant horizons challenging (Evenick, 2008).

Understanding these challenges underscores the necessity for developing necessary interpretation skills. Effective selection and visualization techniques not only aid in capturing subsurface details but also enable accurate interpretations despite the complexities introduced by stratigraphic shifts and discontinuities (Veeken, 2007).

Nonetheless, conventional seismic sections and time slices ‘displays’ typically fail to capture minor faults, which are important in terms of geology or exploration. This is as a result of their smaller throws in comparison to the seismic survey's resolution limit (Iheanyichu and Lawson, 2018). Therefore, the presence of faults can affect the interpretation’s decisions or perceptions. Their significance is related to their role in source and reservoir potentials; and in trapping and migration mechanisms (Evenick, 2008). When faults are mapped, their configuration may be such that they occur as systems of interconnecting faults, dividing the field into several compartments and hydrocarbon zones (Rotimi *et al*, 2010). They may occur scantily or may not be prominent on the seismic sections even though they exist in the field of study. In both cases, locating them successfully is key and may warrant the generation of a seismic attribute especially when poor resolution challenges around sub-seismic faults and within stratigraphic features (like channels) are observed (Iheanyichu and Lawson, 2018).

Despite the generation of this type of attribute, in which the seismic data is transformed into a property that enhances the features of interest, the expertise of the interpreter in pattern recognition and comparison with sub-surface morphological features is very important (Bacon *et al*, 2003; Chopra and Mafurt, 2007). Thus, through seismic attributes one may be able to

extract delicate geologic details from within faults, channels and then predict the structural deformation history. According to Brown (2004), coherence, continuity, semblance, and covariance attributes are all somewhat related. The continuous seismic reflections observed on the seismic sections undergo conversion into a discontinuity volume, effectively capturing and revealing fault lines and boundaries as discontinuities within the attribute volume. These seismic attributes work within a time window and employ various mathematical techniques (Chopra and Mafurt, 2007). The attributes are devoid of interpretation bias because they are directly generated from the processed data (Brown, 2004).

The concluding part of site appraisal should include volumetric and recoverable reserves estimation. Mapped structures and traps need to be assessed (Veeken, 2007). The reservoir rock properties such as porosity, hydrocarbon saturation, closure definition (trap) and volume of the net reservoir obtained from the Net-to-Gross ratio are needed inputs for this assessment in order to quantify the hydrocarbon volume (Adagunodo *et al*., 2022). The time horizons must be depth converted because the fluid contacts represent the lateral definition of the hydrocarbon prospect and their depths are better picked on wells which are recorded in depth (Adeoye *et al*, 2022). Geostatistics and simulations may then be carried out as they give a better comprehension of the risk and amount of uncertainty related to the expected fluid flow behavior in a reservoir. Thereafter, a ranking of the various prospects is usually prepared, taking fully into account the economics of the projects. Finally, a detailed field development plan (FDP) is devised. Overestimating reserves can cause financial strain on a company if production falls short of projected estimates, and it can misguide researchers seeking to comprehend the subsurface occurrence of hydrocarbon accumulations. In cases where calculated reserves appear insufficient, there's a risk of prematurely abandoning or deeming a field unproductive, yet this assessment might not accurately reflect the field's potential.

2. MATERIALS AND METHODS

The analysis began with running a quality check on the log data, by removing spikes from the logs motifs and petrophysical analysis was subsequently utilized to map porous and permeable units using the gamma ray log (GR log), and resistivity logs (RES DEP). The resistivity logs were used to identify the reservoir fluids in order to find the productive reservoirs because log anomalies with high resistivity values indicate hydrocarbon presence. Other petrophysical characteristics of the formations' reservoirs obtained from log interpretation include reservoir lithology, hydrocarbon saturation, porosity, and gross and net thickness of the productive units.

Six distinct types of logs were used in the study, including gamma ray, volume of shale, density porosity, neutron, resistivity, and water saturation logs. Fluid contacts were identified using the overlay of neutron and density porosity logs. In order to estimate hydrocarbon reserves efficiently, the fluid contacts were required on the structure maps. The water saturation equation developed by Archie in 1942 was used to generate the water saturation logs from the resistivity logs. Water saturation (S_w) provides an indication of the degree of hydrocarbon saturation (H_s) through the Schlumberger 1989 formula:

$$H_s = 1 - S_w \quad (1)$$

Afterwards, a synthetic seismogram was created. The generation of the synthetic seismogram is applied for horizon tracking through the seismic lines. During the process of generating the synthetic, a wavelet was extracted from the seismic data. This was afterwards convolved with the reflectivity series obtained from Zoeppritz equation below:

$$\text{Reflectivity Series} = \frac{P_2V_2 - P_1V_1}{P_2V_2 + P_1V_1} \quad (2)$$

Structural modelling process involved positioning picked fault and relevant structural horizons in three dimensions using the application software (*Petrel* TM). Thus 60 seismic inlines and 40 crosslines were interpreted using this procedure. To produce time structure maps, horizon seeds were selected on a grid of inlines and crosslines that encompassed the whole study field. The reflection's amplitude signals were used as guides in order to identify each horizon from one seismic line to another. By doing this, it is ensured that the stratigraphic surface being followed is uniform throughout the region. Since the lateral continuity and dips of events are frequently easier to discern, it was typically desirable to identify seismic horizons on dip lines (Evenick, 2008). The two-way travel times of two (2) horizons were posted and contoured on the base map since each horizon contains reflections that are time-recorded. The *Petrel* TM Software was used to do this. The goal of contouring is to identify the underlying structure from which structural highs and other features that frequently act as potential traps for hydrocarbon-bearing reservoirs can be located (Rachael and Laurence, 2004). The observed faults are noted on each seismic line and linked to one another.

The best technique for modeling faults in the study, was to generate fault sticks from covariance sections. They transform into fault polygons when they are connected from one seismic line to another. However, prior to creating fault polygons, the vertical interval of the fault presence was examined on Covariance attribute maps. The attribute is an estimation of local variance in the seismic signal. It is an edge enhancement method (Chopra and Mafurt, 2007). It was used for imaging discontinuities related to faulting on the seismic data. Eventually, the fault polygons were converted into fault models by the software's modelling module.

Time-to Depth conversion is necessary because during the field development of identified reservoirs, drillers are more interested in depth than in time (Coffen, 1984). To generate a depth map, it is essential to extrapolate data from well sites. This enables the examination of horizon depths laterally within the designated field of study. Depth structure maps were created using average velocities derived from checkshots (Coffen, 1984) since the product of velocity and time yields depth. Thus, a depth map displays the depth to the top of hydrocarbon reservoir. The domain conversion workflow in *Petrel* is a two-step process (Schlumberger, 2013). First, one must define a velocity model derived from the Time- Depth relation (checkshots). This velocity model can then be used to perform domain conversion on the data. According to Veeken (2007), velocity is found to be some relatively simple function of depth that can be expressed analytically in many basins where the succession of lithology is dominated by

alternations of sandstone and shale, such as in the Niger Delta. A linear function of velocity with depth was used:

$V_{(z)} = V_0 + K*Z$ 3

Where: V(z) = velocity at depth Z.

V_0= Datum Velocity

K = velocity gradient with depth

Z= the distance of the point from the datum

The formula above was used to generate velocity models by calculating velocity right from the surface of the earth/datum down to the depth of interest. The velocities are expected to change by a factor of K (the velocity gradient). The Linvel method in Petrel can derive V_0 and K values using Time-depth relations (Schlumberger, 2013).

Volumetric estimation is concerned with quantifying how much oil and gas exists in an accumulation even though volumetric estimates are expected to change over time due to production and recharge (Adeoye *et al.,* 2018). Reserves estimates was done by transferring the oil-water contact (OWC) to the depth structure maps. This contact defines the lateral dimension of the reservoir. Other inputs in the reserves estimation include water saturation (S_w), porosity and gross rock volume; and by using a map-based calculation module in *Petrel's* volume calculation module, these parameters are multiplied together to obtain the Stock Tank Oil in Place (STOOIP). While two primary methods—deterministic and probabilistic—are typically employed for estimating volumetrics, the preference for probabilistic methods arises from their capability to generate a probability distribution of reserves based on the varying input petrophysical data. This method is reliable because each input parameter used for estimating reserves such as net pay, porosity and water saturation has a range of values within the reservoir.

The results were obtained at different probability estimates. In other words, P10, P50 and P90 estimates.

1. (P90): The lowest estimate. It means that 90% of the calculated estimates will be equal or exceed P90 estimate. It is the same thing as proved estimates.
2. (P50): This is the median.
3. (P10): The highest estimate, it means that 10% of the calculated estimates will be equal or exceed P10 estimate. This estimate is categorized as a possible obtainable reserve estimate.

3. RESULTS AND DISCUSSIONS

Figure 1 displays saturated hydrocarbon units in green with their tops and bottoms. The gamma ray log increases and decreases abruptly within the hydrocarbon columns and are therefore interpreted as sand and shale divisions. The hydrocarbon layers also show significant resistivity anomalies within the sands. However, these responses are significantly reduced in reservoir 3, indicating a complicated pore fluid saturation profile. The corresponding low water saturation displayed on the water saturation log (S_w log) supports the interpretation of the resistivity log

(RES_DEP). Water saturation is low and ranges from 25 to 45 percent indicating that hydrocarbon saturation is high.
The hydrocarbon-bearing layer one (1) typically extends from well 1 to wells 3 and 4. The second hydrocarbon unit is only present in wells 1 and 3, and it is not as continuous as the first. Low hydrocarbon saturations are observed in the 3rd reservoir. In addition, high volume of shale (VSH), between 0.61-0.91, is observed within the reservoir, leading to the conclusion that reservoir quality is low.

3.1. Structural Interpretation of Horizon one

There is a complex architecture related to the developments of the faults. The faults are not prominent and can be misinterpreted as non-existent. Fault interpretation was actually difficult on the seismic sections as shown on the diagram. However, through the generation of a seismic attribute (covariance cube), the faults became more prominent and were mapped (Fig. 3). By comparing the seismic section with its equivalent covariance section, the clarity with which the fault patterns stand out, is significant and these would otherwise have been difficult to decipher from the seismic data alone.

Most of the faults are listric normal but do not extend considerably in the vertical direction. The listric faults disappear often on the seismic sections after some lateral distance tracing (Fig. 4). Although structure-building growth faults are prevalent in the Niger Delta, this study did not identify them. The crestal faults noticed were not extensively developed. (Ajakaiye and Bailly, 2002). The little vertical offsets along the faults may assist in fault sealing capability of the fault. Since the faults do not extend much in both vertical and horizontal directions, migration of fluids is probably through seismic or tectonic activities.

On the time structure map (Fig.4), the main faults that penetrated horizon one is located in the Northern and Northeastern part of the field. Other minor faults are observed in the central, southern, and southeastern part of the field. The hanging wall closures formed by the faults dipping in the northeastern direction are the target area for the accumulation of hydrocarbons. This is between contour interval, 2850 ms and 2640ms with the crest of the anticlinal structure located at 2640ms. The corresponding depth structure maps was produced by multiplying the time structure map with the time-depth relation in the equation below:

$$y = 3.72534x + 2568.96 \quad (4)$$

The depth structure map in figure 5 reveal structures similar to those of the time structure map. Anticlines are observed, represented by closures (closing contour lines) within the contour values of 7600 ft and 8500 ft in the Northern and Northeastern section of the field. Due to the upward migrating forces acting on subsurface fluids, hydrocarbon fluids identified from well one (1) can migrate vertically upwards from the point of generation until they are trapped by the limbs of the folded structure (anticline) and vertically by the cap rock and the crest of the anticlinal structure. However, the closures do not close completely because they are terminated by the boundaries of the field of study in the Northern direction. The implication of this is that the full extent and boundary of the anticlinal structure cannot be known from this particular field of study. However, if additional field data is obtained adjacent to the northern section of

the study area, this will reveal the continuity of the trap and the subsequent lateral dimension of the trapping mechanism may increase. The closure identified can impede the vertical and lateral migration of fluid, with the embedding medium (Shale) serving as the seals.

3.2. Structural Interpretation of Horizon two.

The second horizon shows almost the same structural features as the first (Fig. 6). The contour values from 2790ms to 3300ms represents the structural closure entrapping the reservoir. Hydrocarbons have been identified in wells 1 and 3 but as on the first-time structure map, only the hydrocarbon in Well 1 seem to be structurally well located. Well 3 and 5 are located between 3300ms and 3450ms contour lines where synclinal structures (basins) are observed. Any hydrocarbon located in these wells will probably migrate to the structural closure described above if they are not lost during their migration. The diagram also shows that many listric faults are present, totaling 14 faults.

The direct method of time - depth conversion using an equation derived from the check-shot data and time from the time structure map is applied for the depth conversion.

$$y = 0.837447x + 774.647 \quad (5)$$

The depth structure map shows the top of 2nd hydrocarbon trapping mechanism, seen at the ranging depth of 8970 ft to 9,300 ft (Fig. 7). This is the lateral definition of the trapping mechanism. The contour lines between 9300ft to 9450 ft are closely packed, depicting steeping structures. These are the limbs of the anticlinal structure.

Away from the northern and northeastern part of the field, structural low areas are observed in the north western, central and in the southern part of the area. The area shaded from blue to purple fall into this category. These are not good structures for hydrocarbon accumulation because hydrocarbon fluids migrate away from structurally low areas to structurally high zones. Although, closing contours are also observed between 9240 ft to 9300 ft in the south eastern area, but this folded structure is not as high as the trapping mechanisms observed in the northern section. In addition, no wells are drilled around the area for proper identification of oil or gas reservoirs.

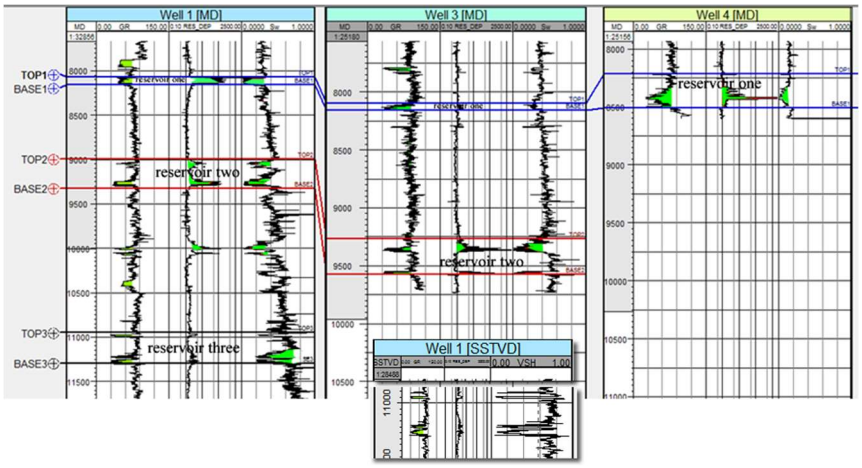

Figure 1: Well Sections showing hydrocarbon zones.

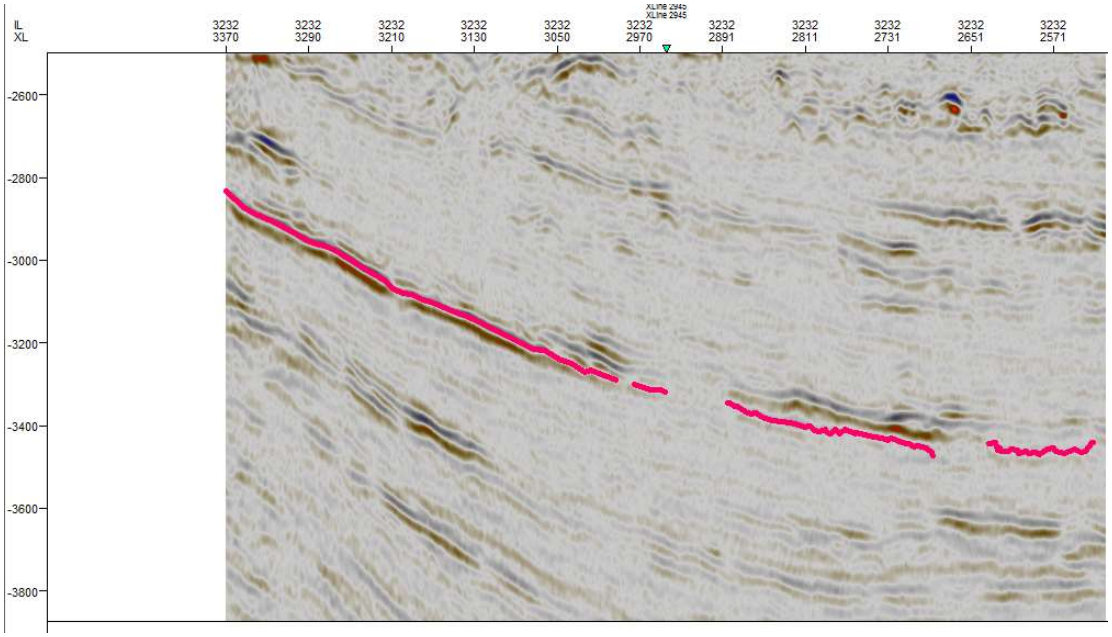

Figure 2: Seismic section showing picked horizon without prominent faults.

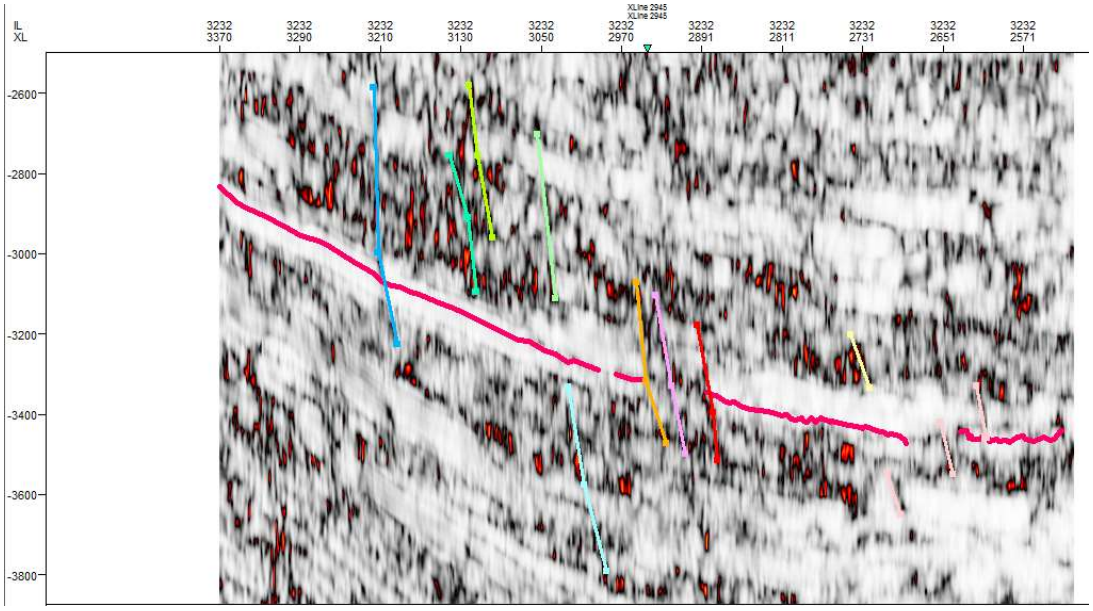

Figure 3: Equivalent Covariance attribute section showing interpreted faults and horizon.

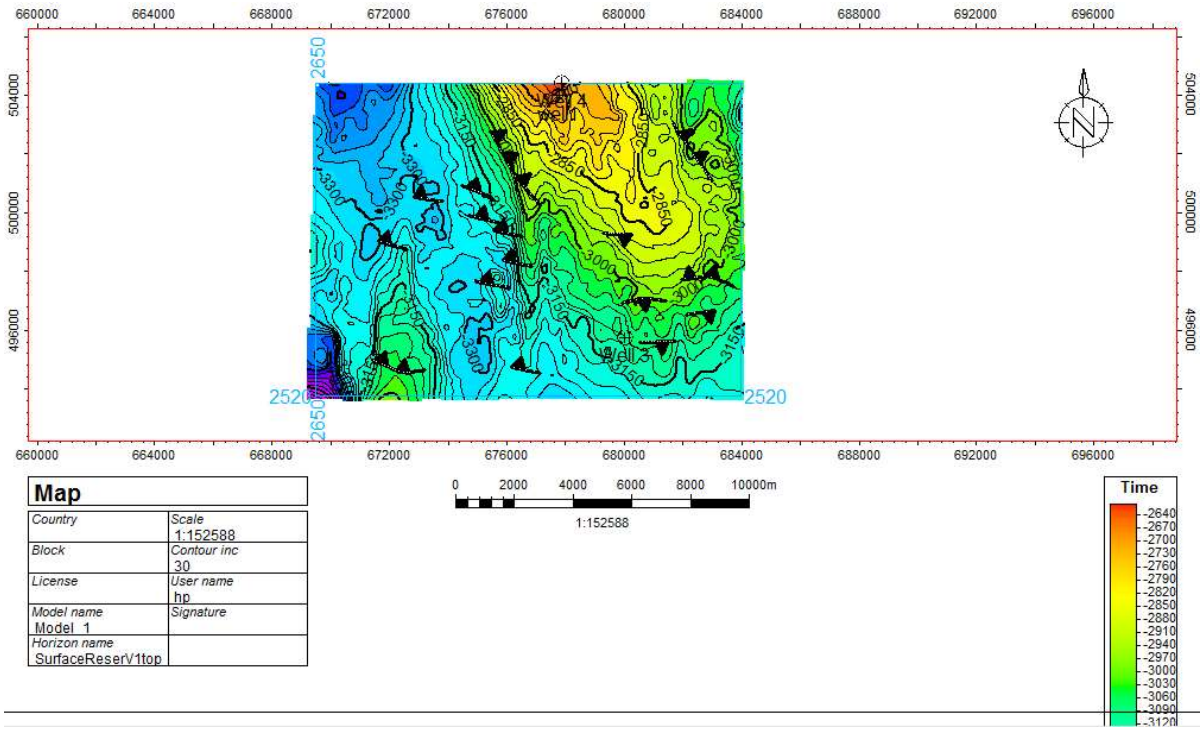

Figure 4: Time Structure map of Horizon one.

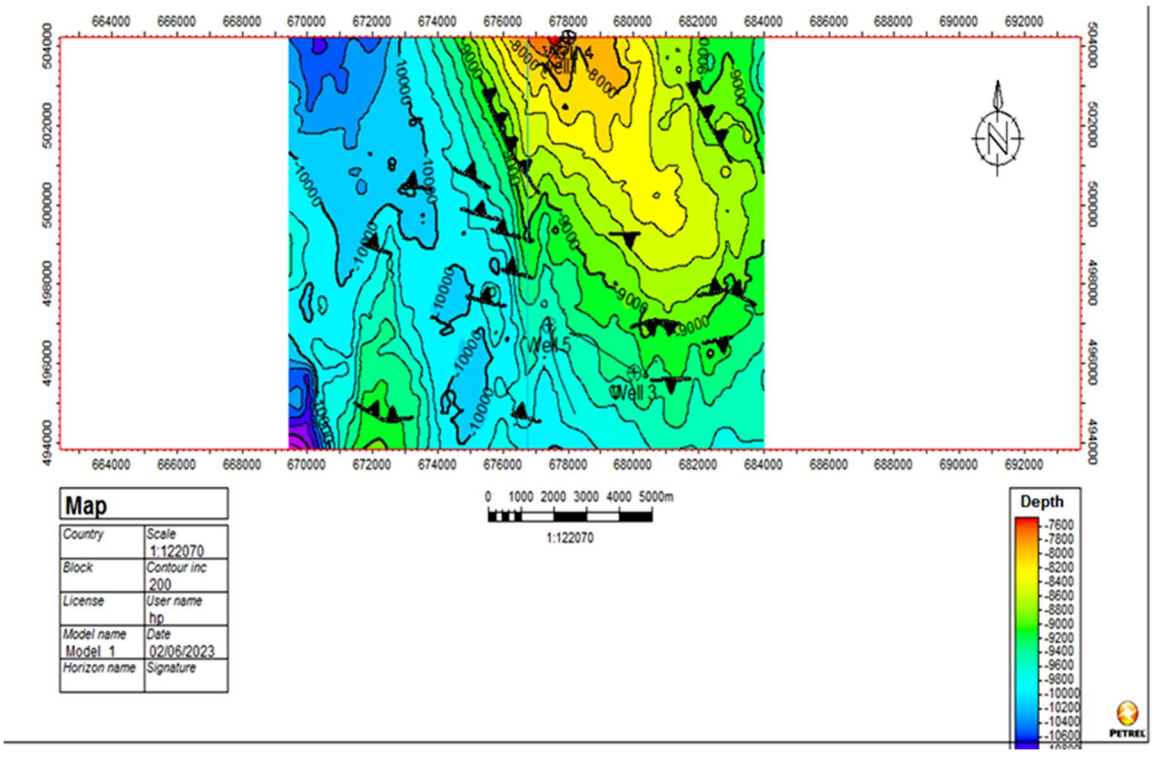

Figure 5: Depth Structure map of Horizon one.

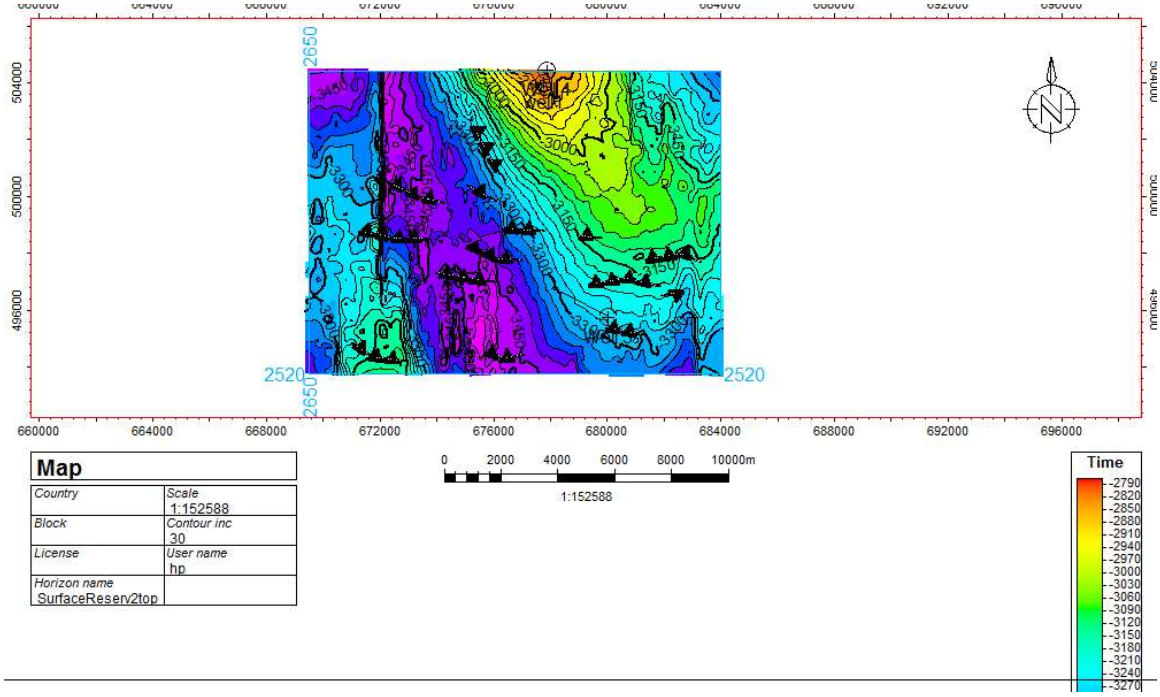

Figure 6: Time Structure Map of Horizon two

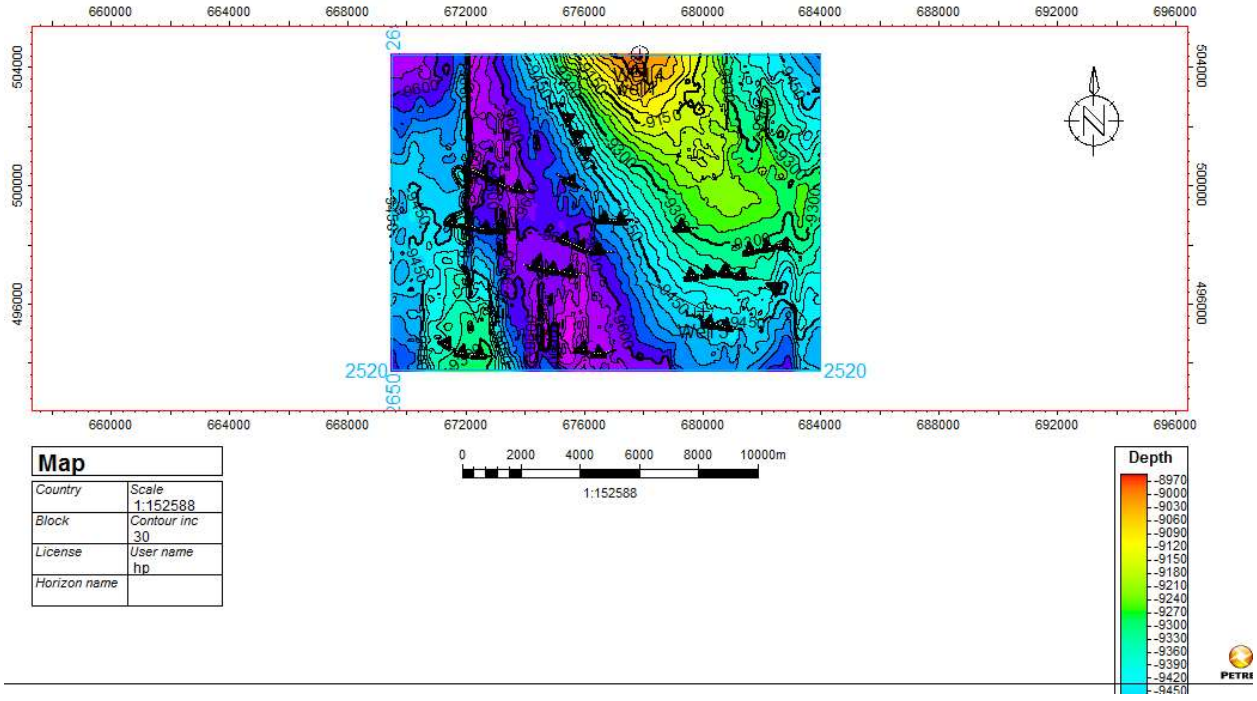

Figure 7: Depth Structure Map of Horizon 2

3.3. Fluid Contact Mapping

Fluid contact mapping is important as its depth corresponds to the lateral dimension of the hydrocarbon reservoir, especially if the reservoir trapping mechanism is an anticline (Evenick, 2008). The reservoir in figure 8 is defined by the oil-water contact observed at the depth of

8154 ft. The measured depth (MD) is shown on the first column and recorded against it are the gamma ray log (Gr), Deep reading resistivity log (RES_DEP), synthetic seismogram (Synthetic 1) and overlay of Neutron and Density porosity logs. The Gr, RES_DEP and synthetic logs are to guide the interpretation such that the contact is indeed picked within the hydrocarbon layer (reservoir 1). The synthetic model shows that the oil-water contact is picked on a low impedance red reflection. The crossing over of the neutron (Neut) and density (Estimated) logs were used to define the oil-water contact.

Figure 9 shows the oil-water contact for the second reservoir at depth 9293 ft. This result agrees with several workers in the Niger Delta who have picked hydrocarbon contact around 8,000 ft – 9, 400 ft (Adagunodo *et al*, 2022, and Adeoye *et al*, 2018). These ranges of values are within the Agbada formation where hydrocarbons are known to be juxtaposed with intraformational seals (Ajakaiye and Bailly, 2002). The contact is picked at the crossing over point of the Neutron and Density Porosity log. It is essential that the crossing over of the two (2) logs do not depict a lithologic effect which occurs most times when the cross overs are observed at a lithological boundary interpreted from the Gamma ray log.

Considering figure 10, the depth to the hydrocarbon-water contact, discussed above is shown, posted on the depth structure map. Positions of initial fluid contacts are critical for field reserve estimates and for field development. This is because the lateral dimension of the hydrocarbon reservoir is obtained from it, measured up to the peak of the anticlinal structure (Coffen, 1984). In contrast to the dimensions deduced from the trapping mechanism on the depth structural maps, the reservoir area reduces to the area shaded in green. The reduction of the reservoir area then means that the oil fluids do not fill the entire anticlinal structure. However, this reservoir dimension may increase if the area covered by the seismic data is known in the northern part of the study area.
In Figure 11, the oil-water contact is shown on the depth structure map for the second reservoir. It is depicted by a green color fill in the Northern section of the study area. This diagram shows how the unit's lateral dimension has grown. The interpretation deduced is that at the fluid contact depth of 9293ft, the lateral dimension of the hydrocarbon column has increased.

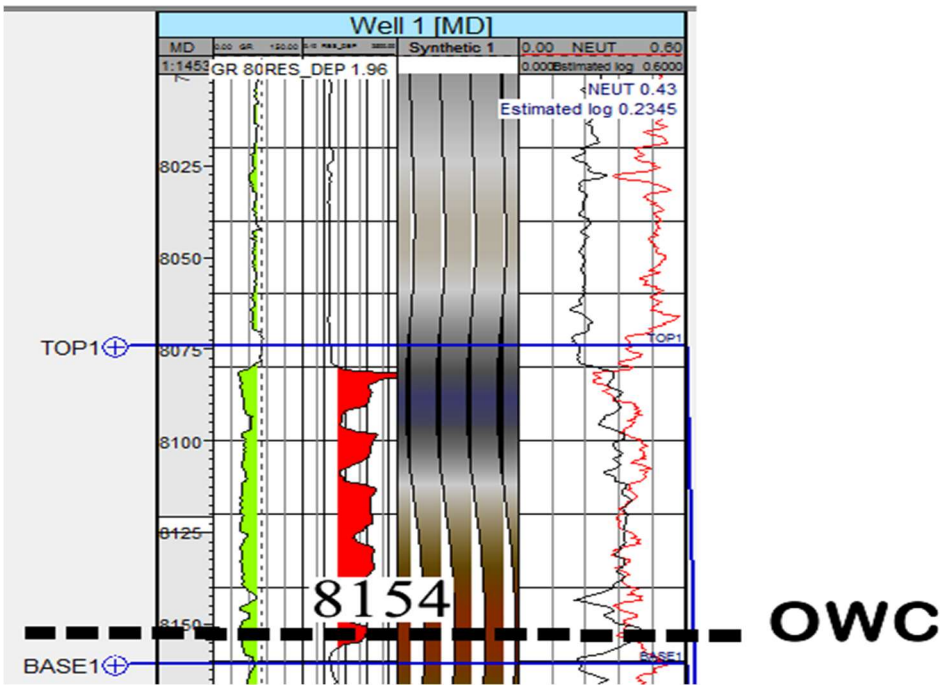

Figure 8: Delineated oil water contact (OWC) in Reservoir 1.

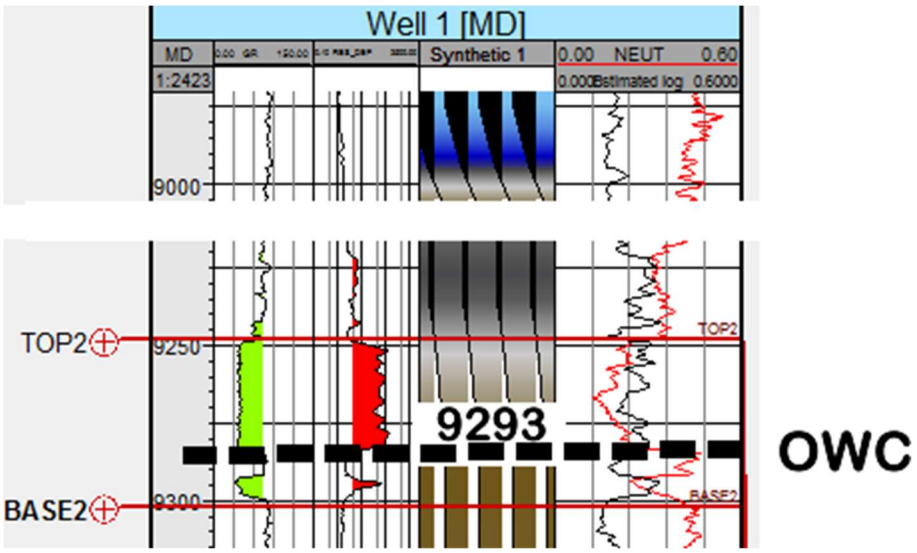

Figure 9: Delineated oil water contact (OWC) in Reservoir 2.

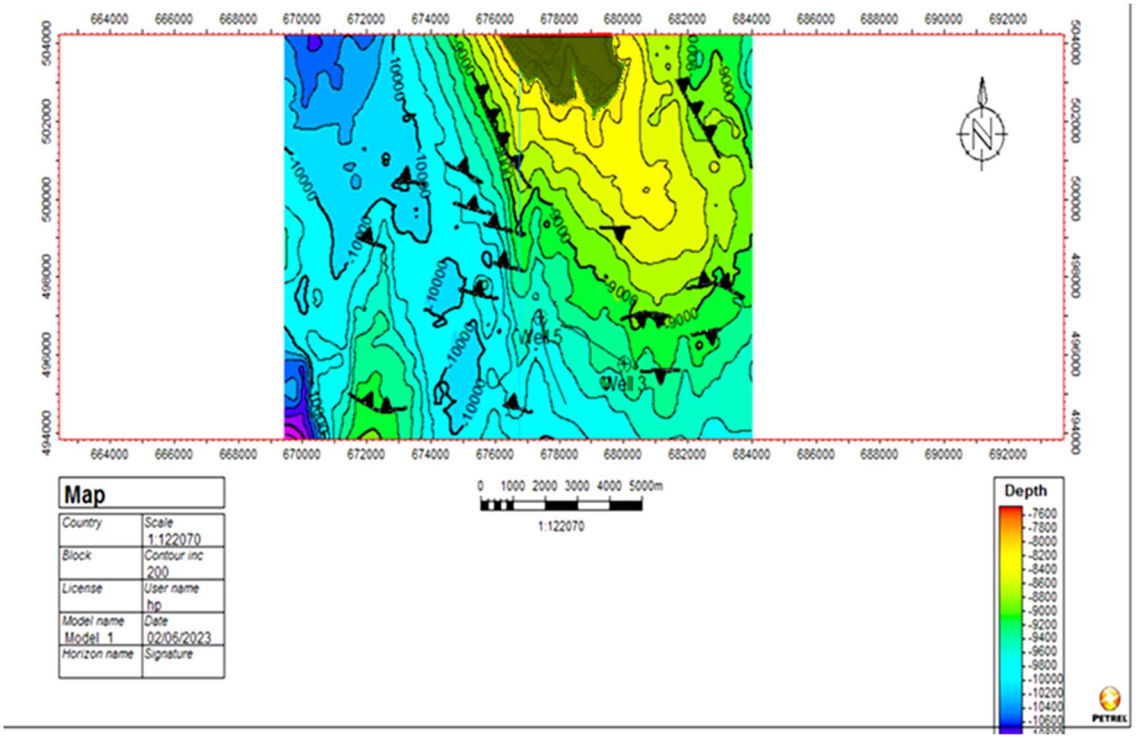

Figure 10: Oil-water contact of reservoir one posted on the depth structure map of horizon one.

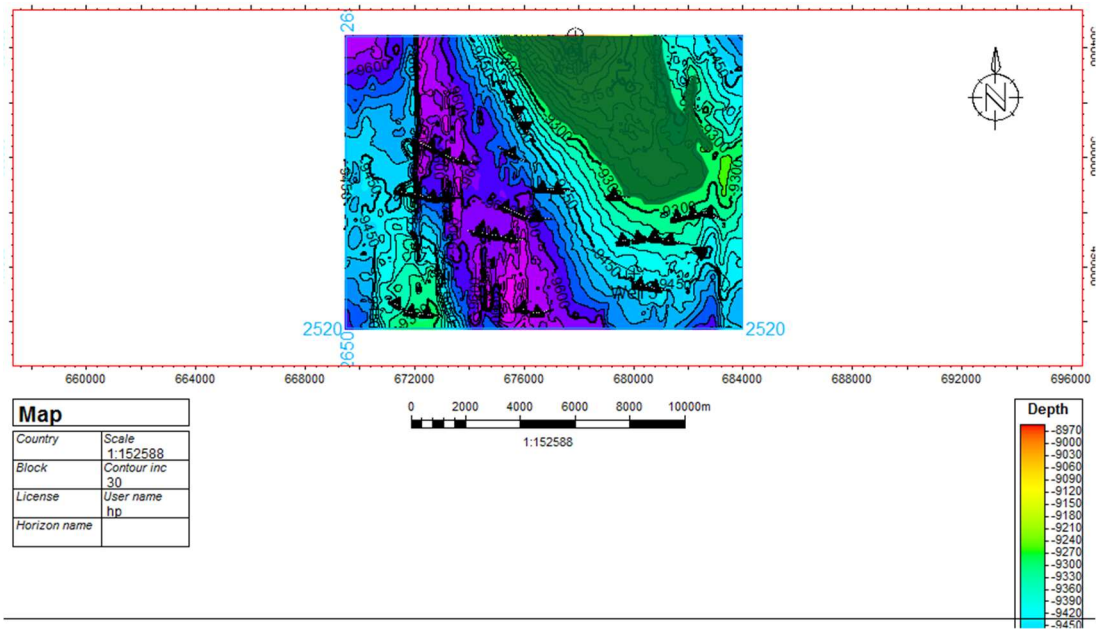

Figure 11: Oil-water contact of reservoir two posted on the depth structure map of horizon two.

3.4. Reserves Estimation Results

Table 1 shows the estimate of the oil reserves from reservoir one (1). The reserve estimates change as the water saturation value changes. In optimistic (P10%), median (P50%), and pessimistic (P90%) scenarios, variations occur in the lateral and vertical Net-to-Gross, porosity, and hydrocarbon saturation (Table 4.1). At the end of the analysis, a value of 524,

235 barrels of oil was estimated from reservoir one (1) at the P10 confidence level. This means that 524, 235 barrels of oil is the highest oil reserves obtainable from reservoir 1 but that there is a low probability (10%) that this estimate will actually be obtained. The lowest volumetric estimate that is possible is 333,333 barrels but there is a high (90%) probability that this quantity of reserves will be produced. Taking an average of P10, P50 and P90 volumetric estimates, 394,192 barrels of oil can be produced with an assumed recovery factor of 30%. This value is adjudged to be quite low, when compared with what is generally obtainable in the Niger-Delta.

Using the porosity values, hydrocarbon saturation (S_w), Net-to-Gross and other properties, volumetric results is shown for the second reservoir in Table 2. The table shows overall summary of the petrophysical analysis of reservoir two at the various uncertainty levels (P10, P50 and P90 confidence levels). The obtainable quantity of oil increases drastically, probably because of increase in the size of the reservoir area. Assuming a recovery factor of 30%, the reservoir has the potential to yield a significant amount of oil, with an average production estimate of 1,120,779 barrels.

Table 1: Table showing reserves estimates and reservoir parameters in reservoir one

RESERVOIR 1	CONFIDENCE LEVEL	TOP (ft)	BOTTOM (ft)	GROSS THICKNESS (ft)	NET THICKNESS (ft)	N/G	POROSITY	AREA (acres)	HYDROCARBON SATURATION	OIL RESERVES (BARRELS)
1	P10	8076	8156	80	76	0.95	0.32	388.63	0.75	524,325
2	P50	8070	8144	74	70	0.95	0.30	345.01	0.65	415,010
3	P90	8055	8127	72	68	0.94	0.22	333.25	0.55	333,333

Table 2: Table showing reserves estimates and reservoir parameters in reservoir two.

RESERVOIR 2	CONFIDENCE LEVEL	TOP (ft)	BOTTOM (ft)	GROSS THICKNESS (ft)	NET THICKNESS (ft)	N/G	POROSITY	AREA (acres)	HYDROCARBON SATURATION	OIL RESERVES (BARRELS)
1	P10	9001	9594	593	467	0.78	0.24	814.12	0.85	1,444,301
2	P50	9533	9681	148	111	0.75	0.22	731.44	0.67	1,217,023
3	P90	9601	9700	99	68	0.69	0.19	600.23	0.55	701,012

4. CONCLUSIONS

The study details the varying quality of reservoirs and their hydrocarbon saturation across different wells. The identification of hydrocarbon tops and bottoms from well log analysis

revealed three (3) hydrocarbon reservoirs occurring mostly within shaly sands. The interpreted oil sands were identified in well 1, 3 and 5, which are far apart. The structural interpretation of the fault architecture reveals challenges in fault identification and the significance of seismic attributes in fault mapping. The trapping mechanism identified for the reservoirs are fault bounded anticlinal structures located in the Northern part of the study area. The depth of the trapping mechanism ranges between 7600ft and 8500 ft for Reservoir 1. Reservoir 2 spans from 8970 feet to 9300 ft. Structure maps were not generated at reservoir 3 level because of its low hydrocarbon saturation and high volume of shale. Covariance attribute analysis show that the study area contains many normal listric faults that are not extensive in the vertical and lateral direction and are mostly not connected to each other. Oil sands may move to well 1 area unhindered because the structural peak is located at the region. It is possible that further oil migration will be lost beyond the aforementioned trap region. On the depth structure maps, fluid contact mapping was accurately done using neutron-density overlays, and oil-water contact was picked at the depth of 8,154 ft and 9,293 ft respectively.

The Reserve Estimate indicates an oil volume ranging from 333,333 to 1,444,301 barrels. The estimated hydrocarbon content in the first reservoir averages 394,192 barrels, while the second reservoir boasts a significantly higher volume, averaging 1,120,779 barrels representing a substantial potential for generating returns on investment. In addition, obtaining more data could expand the size of the anticlinal structure in the northern section, potentially augmenting hydrocarbon reserves because the prolific structure did not close completely around that area.

REFERENCES

Adagunodo, T. A., Bayowa, O. G., Alatise, O. E., Oshonaiye, A. O., Adewoyin, O. O., and Opadele, V. O., (2022). Characterization of reservoirs and depositional study of JP Field, shallow offshore of Niger Delta Basin, Nigeria, *Scientific African*, *15*.

Adeoye, T. O., Sunmonu, L. A., Adabanija, M. A. and Bayowa, O. G., (2022). Fluid Substitution - Based Reservoir Studies and Seismic Response in 'Vyshion' Field, Niger Delta. *Ilorin Journal of Science,* 9 (1) 70 – 85.

Adeoye, T. O., Raji, W. O. and Ibrahim, O.K., (2018). Hydrocarbon reserve estimates and risks assessment in 'X' ray field, Niger Delta, Nigeria. *Adamawa State Univ. J. Scient. Res.*, 6 (1) 32-45.

Adeoye, T. O., Ologe, O., Johnson, L. M., and Ofomola, M. O., (2017). Shaly sand analysis From well logs: Case study of a Niger Delta Field, Nigeria. *J. Pure and Appl. Sci.*, *30* (3) 3074-3084.

Ajakaiye, D.E., and Bailly, S., (2002). Course manual and atlas of structural styles on reflection profile from Niger-Delta: *American Association of Petroleum Geologists, Tulsa, Oklahoma*. pp. 1-42

Archie, G.E., (1942). The electrical resistivity log as an aid in determining some reservoir characteristics: *Journal of Petroleum Technology*, 5, 54-62.

Ashcroft, W., (2011): *A petroleum geologist's guide to seismic reflection*, 1st edn., John Wiley & Sons, West Sussex, United Kingdom, 55.

Bacon, M., Simm, R. and Redshaw, T., (2003): *3-D Seismic Interpretation*, 1st edn.,

Cambridge University Press, New York, 146-148.

Brown, A. R., (2004): *Interpretation of three-dimensional seismic data*, 6th edn., American Association of Petroleum Geologists, Memoir 42, Oklahoma, U.S.A., 153-160.

Chopra, S., and Marfurt, K. J., (2007). Volumetric curvature attributes for fault/fracture characterization. CSPG CSEG convention, *first break*, *25* (1109).

Coffen, J.A., (1984). Interpreting seismic data: Penwell Publishing Company, Tulsa Oklahoma. pp. 39-118.

Evenick, J.C., (2008). Introduction to well logs and subsurface maps. 1st edn. Pennwell Corporation. Okhlahoma, USA. 41-72.

Iheanyichu, O. A., and Lawson, O., (2018). 3-D Seismic Attribute Analysis for Enhanced Prospect Definition of" Opu Field", Coastal Swamp Depobelt Niger Delta, Nigeria. *Journal of Applied Sciences*, *18* (2) 86-102.

Rachael, T., and Laurence, R., (2004). Fundamentals of Geophysical interpretation: SEG Geophysical monograph series. No. 13, pp 23-213.

Rotimi, O. J., Ameloko, A., and Adeoye, T. O., (2010). Applications Of 3-D structural interpretation and seismic attribute analysis to hydrocarbon prospecting Over X–Field, Niger- Delta. *International Journal of Basic & Applied Sciences*, *10*(4) 28-40.

Schlumberger, (2013). Petrel Geophysics – Seismic Visualization and Interpretation training And Exercise Guide. Schlumberger E & P Software Platform, 2013. pp 341-375.

Schlumberger, (1989). Log Interpretation, Principles and Application: Schlumberger Wireline and Testing, Houston, Texas. p 21-89

Veeken, P.C.H., (2007): *Seismic stratigraphy, basin analysis and reservoir characterization. Handbook of Geophysical exploration*, 37, 1st edn., *Elsevier,* Oxford, United Kingdom, 388.